Potential of Oxygenated Palm Stearin Wax- An Agricultural Waste as Biofuel in a CI Engine – An RSM Approach

Hariram V*‡, Allen Jeffrey J**, Sangeethkumar E***, Christu Paul R***, Adam Hashim Dalal***, Shweta Sunil Menon***, Vinoth Kumar M*, Godwin John J***

*Department of Mechanical Engineering, Hindustan Institute of Technology & Science, Padur, Chennai

**Department of Mechanical Engineering, Loyola Institute of Technology, Palanchur, Chennai

***Department of Automobile Engineering, Hindustan Institute of Technology & Science, Padur, Chennai

(connect2hariram@gmail.com, jeffyresearch@gmail.com, esangeethk@hindustanuniv.ac.in, rchristu@hindustanuniv.ac.in, adamhdalal@gmail.com, menonshweta2214@gmail.com, mvinothk@hindustanuniv.ac.in, godwinjohn18@gmail.com)

‡ Hariram V, Department of Mechanical Engineering, Hindustan Institute of Technology & Science, Padur, Chennai, Tamil Nadu, India, Tel: +8939092346

connect2hariram@gmail.com

Received: 26.05.2022 Accepted: 01.08.2022

Abstract- This experimental investigation is aimed at evaluating the ideal engine operating parameters related to the emission and performance aspects of a compression ignition engine by deploying Response Surface Methodology (RSM). A four stroke 5.2 kW naturally aspirated water cooled compression ignition engine fuelled with oxygenated blends of palm stearin biodiesel was used in this study. Single stage base catalyzed transesterification process using methanol and NaOH produced biodiesel. The input operational parameters were the test fuel blends (FB), compression ratio (CR) and engine load (EL) while the output responses were brake specific fuel consumption, brake thermal efficiency and exhaust emission comprising unburned hydrocarbon, carbon monoxide, oxides of nitrogen, carbon dioxide and smoke emissions. A 3x3x3 full factorial RSM design matrix based on central rotatable composite design (CCRD) was developed to assess the suitability of oxygenated palm stearin biodiesel in CI engine. Analysis of variance was used to evaluate the RSM model based on the goodness of fit values. Increased DEE concentration to diesel biodiesel blends augmented 41.78% at 3/4th loading conditions. Optimal BSFC was observed to be 0.285362 kg/kWhr based on compression ratio 18:1 at 9.55229 kg engine load for D80PSBD20DEE10 fuel blend. RSM predicted a superior BTE of 40.5663% when D80PSB20DEE10 fuel blend was used in CI engine at compression ratio 18:1 and 9.55229 kg of engine load. Optimal concentration of UBHC and CO was seen at CR18:1 for oxygenated fuel blends at 9.55229 kg engine load. Considering the desirability value and RSM prediction, the optimal input operation parameters were CR18:1, D80PSBD20DEE10 blend and 9.55229 kg of engine load. The optimal output response for BTE, BSFC, CO, UBHC, CO_2, NO_x and smoke were 40.5663%, 0.295362 kg/kWhr, 0.27002%, 73.65 ppm, 506.32 g/kWhr, 735.721 ppm and 87.9334% respectively. The outcomes of the RSM prediction suggested that it is a reliable and powerful tool in optimizing the engine's operational parameters to maximize the performance with minimal emissions when fuelled with oxygenated biodiesel blends.

Keywords: Biodiesel, Optimization, Response surface methodology, Performance and Emission, Transesterification

1. Introduction

The rapid diminishing rate of fossil reserves in today's world due to increased use of automobiles and other vehicles and increased vehicular exhaust emissions are the serious concerns in the present environmental-energy scenario [1]. Rapid growth of industrial and transportation sectors in the developed countries compounded serious crisis to the living ecosystem. The energy requirements for the world's growing population are ever increasing day by day. This has led to the

emergence of alternate fuels namely biodiesel from vegetable sources and animal fats [2]. But, extraction of bio-oil from non-edible feedstock is always a challenging task as it should not compete with the edible food crops so that it will not raise negative concerns to mankind. On the other hand, converting the residual solid materials and wax from edible and non-edible vegetable feedstock has gained importance as a value addition aspect.

Globally, Asian countries, especially Indonesia and Malaysia account for nearly 84% of palm oil production followed by South America and Guatemala. Nearly 74 million tonnes of palm oil is produced in the world during through which nearly 15.5 million tonnes of palm stearin wax is derived. This palm stearin wax could be a promising feedstock for the bio-fuel production and also adding value to countries economy [3]. On the other hand, use of diesel - biodiesel blends in the compression ignition engine has witnessed significant reduction in UBHC, smoke and CO emissions along with enhanced engine performance. The combustion aspects of the CI engine which includes the in-heat release rate and cylinder pressure also improved significantly leading to a superior engine output [4]. Increase in the oxygen content of biodiesel-diesel blend using additives along with in-cylinder variation attributed the combustion and performance with further reduction in the exhaust emission [5, 6]. In this scenario, optimizing the engine's output with multiple variation in the input parameter can be understood better by employing soft computing statistical tool which analyze the synergetic effect of various input parameters and helps the researchers to arrive at a conclusion with practical and sustainable outcomes [7].

Many researchers had studied on the usage of palm stearin biodiesel in compression ignition engine. Ambarish and Mandal [8] derived the biodiesel from palm stearin wax through transesterification method. The biodiesel was blended with ethanol / methanol and assessed for the engine combustion phenomenon. Ganesh et al. [9] prepared the biodiesel from palm stearin bio-oil through base catalyzed transesterification method using methanol and NaOH at a oil to molar ratio of 7:1. The emission analysis exhibited a promising reduction in CO and UBHC emissions when CI engine was fuelled with PSME20 blend. Pali Rosha et al. [10] produced biodiesel from palm oil using a batch type reactor. Single stage transesterification process transformed the palm oil into its methyl ester at molar ratio of 10:1, 60℃ reaction temperature, and 1.4 wt% of KoH catalyst concentration for 60 minutes reaction duration.

Numerous studies were performed by the researchers in evaluating the engine's emission and performance criteria when fuelled with biodiesel-diesel-oxygenated blended fuels at various proportions. Higher EGT was showcased due to more quantity of fuel burning by Prakash et al. [11]. A significant reduction in engine exhaust especially CO was noticed along with a notable rise in smoke opacity. The upsurge in fuel blend ratio amplified the BTE and BSEC significantly along with notable reduction in smoke emission. The effect of higher DEE content in kerosene-diesel fuel blend was reported by Patil and Thipse [12] in order to understand the adulteration effect. DEE 10-30% along with 5-15% EGR reduced the NOx and smoke emissions simultaneously. Addition of DEE by 20% gave an optimum performance for the CI engine [13]. Higher blend of DEE (above 30 vol.%) to diesel and biodiesel blend emitted enormous amount of smoke than other test fuels which was due to the phase separation resulting in poor combustion. Few studies also reported on evaluating the CI engine by varying its input operational parameters like fuel injection time, injection pressure and compression ratio. Muralidharan et al. [14] assessed the effect of variable compression ratio engine using blends of waste cooking oil with diesel fuel. The CR was fixed as 21 for all loading conditions. Higher CR reduced the UBHC and CO emissions along with the significant escalation of Oxides of Nitrogen emission. Vikas et al. [15] reported on the usage of bio-mix methyl ester-diesel blends on a 3.7kW VCR CI engine when the compression ratio was fixed as 17.5:1. The amalgamation of karanja, jatropha and cotton seed oil and its esterification process was studied in detail. The biodiesel feedstock quality and the optimized transesterification input process parameters were the main limitations of the study. The compression ignition engine was originally designed for using diesel fuel as the primary feedstock. Now-a-days, the usage of alternate resources like vegetable oil along with variable engine input parameters like in-cylinder pressure, injection timing and compression ratio altered the engine output. But, optimizing the engine performance with respect to the recent advancements is more arduous and costlier. Many researchers had attempted to augment the variable input factors of the compression ignition engine employing RSM technique. Using RSM methodology, Sakthivel et al. [16] studied the engine variable optimization process when using the waste biomass pyrolysis oil. RSM based multiple regression model predicted the emission and performance parameters. Experimental validation revealed that the influence of CR, IT and fuel blend impacted the engine output with an error deviation of less than 5%. Mustafa et al. (2020) optimized the test engine using a combination of RSM and ANN methodology when assessing the performance and emission of CI engine fuelled with biodiesel-diesel blends. The ANN model and RSM model were developed using feed forward multilayer network and quadratic regression respectively. Datta et al. [17] investigated the synergetic consequence of compression ratio and fuel blend of a CI engine when fuelled with palm biodiesel-diesel-methanol fuel blends in variable proportions using RSM. Using RSM, the impact of fuel injection parameters inside the combustion chamber of the CI engine when fuelled with blends of pongamia biodiesel was reported by Pandian et al. [18]. Amged et al. [19] noticed that by using Rapeseed oil methyl esters in combustion with advancement, it decreased the BSFC up to 3.7 at high load and 17.8% during the low load. Hayder et al. [20] evidently found in this research that while using 100% biodiesel the cylinder pressure and rate of heat release slightly increased and also it was noted that particulate size got decreased by 26nm while using B100. Mohammed et al. [21] proved that EGR is an efficient technology to reduce the NO_x emissions drastically. The study was also focused on the effects of oxygenated concentration in diesel blends which significantly reduced the PM concentration.

The literatures enlisted above had independently assessed the influence of using biodiesel-diesel-oxygenate blend in CI engine and further approaches were attempted on analysing the optimization strategies on the engine parameters using soft computing tools. However, the combined effect of oxygenated diesel-biodiesel blends on the optimized engine input parameters of a CI engine using RSM was not attempted. Considering this as a research gap, the present experimental investigation attempts to derive the biodiesel from waste palm stearin wax to make it as a value added product and to understand its effect on the CI engine along with an oxygenated additive. Further, the RSM approach optimizes the engine operating parameters to obtain minimal emissions with maximum performance which was further validated experimentally. Hence the main aim of this investigation was to determine the potential effect of Palm Stearin biodiesel and to optimize the paratmeters using RSM tool. Further improvemnts in the engine's behavioir was evidenced with the addition of oxygenated addivives.

2. Materials and Methods

2.1. Materials

The feedstock for biodiesel production was Palm stearin wax (refer Figure1A), a residue which was the left-over by product during the refining and filtration of palmolein oil in mass fractions. It was developed as a re-crystallization product during the high temperature filtration of palmolein bio-oil. It was considered as a bio-waste and find minimal application in the cosmetic industries. Pure methyl alcohol of 99% purity and sodium hydroxide were used as base and catalyst during the transesterification process. These were procured from Sri Kailash Chemical, Chennai, Tamil Nadu, India. All the biochemical substances employed in this experimental study were of analytical investigative grade.

2.2. Biodiesel Production

The solidified palm stearin wax was brought to liquid form by heating it up to 90ºC for 30 minutes in a glass beaker to produce liquefied palm stearin bio-oil (refer Figure 1B). Phenolphthalein based titration method was carried out on the liquefied palm stearin bio-oil which indicated the free fatty acid content to be 1.73%. Based on this, single stage base catalyzed transesterification process was adopted (refer Figure 1C). Initially, 0.54 wt.% of NaOH pellets was thoroughly mixed with 100 ml of methanol in a glass container at 60ºC for 20 minutes for the formation of sodium methoxide solution as suggested by Amged et al. [19]. Flat bottomed Erlenmeyer flask of 1000 ml capacity which was equipped with magnetic stirrer, heating and temperature adjustment was deployed for the transesterification process. 500 ml of pre-heated palm stearin bio-oil was poured into the flask and agitated at 350 rpm. Sodium methoxide solution was then mixed thoroughly with the palm stearin bio-oil in the Erlenmeyer flask. The transesterification process was maintained at an agitation speed of 450 rpm for 120 minutes between the reaction temperature of 65ºC and 70ºC. The resultant mixture was transferred into a separating funnel after the reaction period and 6 hours of settling time was allowed. Two distinct layers with a separating ring formation at the center of the funnel indicated the completion of the transesterification reaction [23]. Palm stearin biodiesel occupied the upper layer while glycerol, the by-product of the chemical reaction occupied the bottom layer. The rotating knob in the bottom of the separating funnel removed the glycerol, catalyst and methanol. Then, 50 ml of double distilled water was added to the palm stearin biodiesel to remove excess methanol and other impurities. The derived palm stearin biodiesel was heated up to 90ºC for 20 minutes for the removal of moisture content. By this method, 685 ml of palm stearin biodiesel was obtained at a transesterification efficiency of 96.5% (refer Figure 1D).

2.3. Test Fuel Formulation and Its Physio-chemical Properties

In this investigation, one binary and one ternary test fuels were prepared based on the volumetric ratios. In the binary blend, 80% of mineral diesel was mixed with 20% of palm stearin biodiesel and it was named as D80PSBD20 whereas, the ternary blend contained of commercial diesel (72.72%), palm stearin biodiesel (18.18%), DEE (9.09%) and designated as D80PSBD20DEE10. In both test fuels, the volumetric ratio of diesel and biodiesel was kept constant and the effect of oxygenate was assessed in the ternary blend. Mineral diesel was fuelled in the test engine at all experimental conditions to obtain the reference data. All the test fuels prepared were safely stored in darkness for four days before the engine run, to observe the occurrence of phase separation which was not evidenced during this study. The physiochemical properties of palm stearin wax, its biodiesel and blended fuels are tabulated in Table 1. The density and kinematic viscosity of palm stearin wax reduced up to 0.881g/m^3 and 2.41mm^2/s from 0.941g/m^3 and 5.27mm^2/s respectively through transesterification process to make it suitable for its usage in the CI engine. Blending PSBD with mineral diesel and DEE escalated the values marginally. The calorific value of D80PSBD20 was found to be 40329kJ/kg which increased to 42957kJ/kg upon addition of oxygenate. All the physiochemical properties were estimated based on the ASTM standards and it was found to be within the limits.

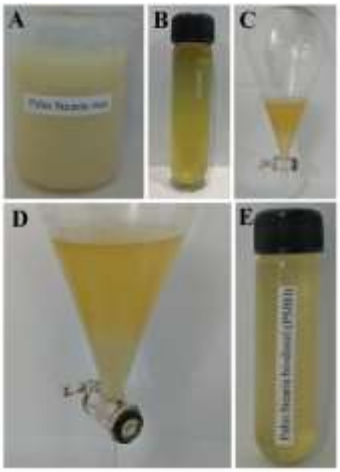

Fig 1. Palm stearin wax (A), palm stearin bio-oil (B), transesterification process(C, D) and Palm stearin biodiesel (E)

Table 1. Palm stearin wax, biodiesel and test fuels – Physiochemical properties comparison

Properties	Palm stearin wax	PSBD	Mineral diesel	D80 PSBD20	D80 PSBD20 DEE10	ASTM standards
Density @ 15°C (g/m^3)	0.941	0.881	0.832	0.841	0.8565	D5002-94
Kinematic viscosity @ 35°C (mm^2/s)	5.27	2.41	2.57	2.45	2.57	D445
Calorific value (kJ/kg)	21543	37122	42955	40329	41845	D4868
Flash point (°C)	-	164	48	127	139.7	D93
Fire point (°C)	-	242	140	168	82.1	D92

Table 2. List of instrument and its uncertainties

Parameters	Measuring range	Accuracy	Uncertainty (%)
Load sensor (kgs)	0-50	±0.1	0.2
Air flow measurement (mm)	0-200	±1	0.5
Fuel flow measurement (mm)	0-500	±1	0.5
Speed measurement (rpm)	0-2500	±10	1
UBHC (ppm)	0-20000	±10	0.2
CO (%)	0-10	±0.02	0.2
NO_x (ppm)	0-5000	±10	0.3
CO_2 (%)	0-20	±0.01	0.2

Table 3. Input variable parameter

Parameters	Levels		
	1	2	3
Compression ratio (CR)	17	17.5	18
Test fuel blends (FB)	D100 (0)	D80PSBD20 (1)	D80PSB20DEE10 (2)
Engine load (EL)	No load (0 kg)	Part load (6 kg)	Full load (12 kg)

3. Experimental setup

Kirloskar TV1 four stroke, single cylinder naturally aspirated water cooled test engine was used in this experimental investigation. The bore and stroke length of the engine was 87.5mm and 110mm respectively. The factory set compression ratio was 17.5:1 which can be varied between 12 and 18 by adjusting the tilting mechanism present near the cylinder head of the engine during working condition. The graduations present near the cylinder head designated the compression ratios of the engine. The exhaust emissions were measured using AVL Digas 444 equipment and the smoke emission was measured using AVL 437 smoke meter. The loading of the engine was carried out using an eddy current dynamometer. The injection timing and pressure was 23°bTDC and 210 bar respectively. The smoke opacity was measured using AVL 437 smoke meter while the CO, UBHC, CO_2 and NO_x emissions were determined using AVL 444 Digas analyzer. The detailed specification of the emission measuring devices and test engine are tabulated in Table 4. Before the start of the engine, the lube oil temperature and coolant flow was checked to ensure safety. Initially, the engine was allowed to run at factory set compression ratio (17.5:1) with mineral diesel for 15 minutes at all loads to attain stability. On reaching steady state condition, the time taken for 10cc fuel consumption was recorded using stop watch at no load, part load and full load operations.

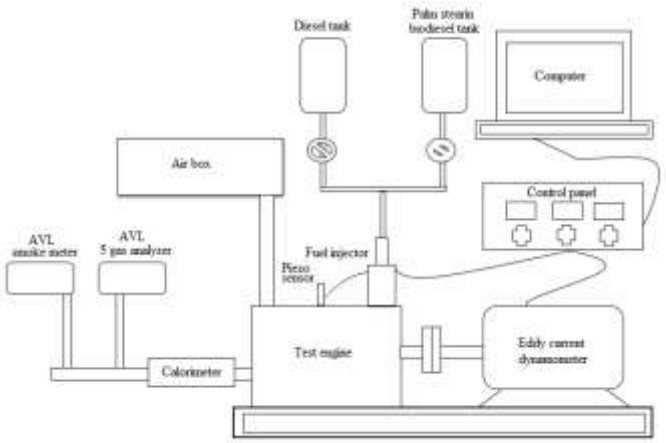

Fig.2. Experimental setup - Schematic

The test fuels namely D80PSBD20 and D80PSB20DEE10 were then admitted inside the engine through a separate bio-fuel tank arrangement as shown in Figure 2. Before the start of every experimental run, it was ensured that mineral diesel was fuelled to the engine in order to remove the residues in the fuel line. AVL444 Digas analyzer and AVL437 smoke meter were allowed to warm-up before the measurement of exhaust emissions. Leak test was initiated by passing the gas into the exhaust lines which was followed by residual test to ensure the absence of hydrocarbons in the tail pipe. The sensing probe of the AVL devices was placed at appropriate positions after passing the preliminary test to analyze the exhaust gases.

Table 4. Specification of test engine, combustion analyzer and exhaust measuring devices

Test engine	
Engine Make and model	Kirloskar TV1
Compression ratio	Variable (12 to 18)
Stroke	110 mm
Injection timing	23ºbTDC
Bore	87.5 mm
Loading	Eddy Current dynamometer
Swept volume	661.45 cc
Rated speed	1500 rpm
Cooling system	Liquid cooled
Gas analyser	
Model and Make	AVL 444 / Digas
Type	110V-220V
Response time	T95 ≤ 15S
Smoke meter	
Model	AVL-437 smoke meter
Measuring range	0-100% opacity
Heating time	20 min (max)
Light source	12V/5W halogen lamp

Errors and uncertainties were inherent in experimental analysis. It was essential to assess the uncertainty of conducted experiments to ensure its accuracy. Error and ambiguities may arise during measurement and calculation. In the present study, root mean square method suggested as by Jeyaprakash et al. [20] was used to assess the uncertainties and the overall value was found to be ±1.43%. The detailed errors and accuracy of the equipment used in this study are tabulated in Table 2.

4. RSM Model Development

Response surface methodology (RSM) was used in the present investigation to assess the engine optimization condition based on the input variable parameters. Three input variables considered in this investigation were compression ratio (CR), test fuel blends (FB) and engine load (EL) as tabulated in Table 3. Based on the literature, the output responses which had a significant effect on variations of the input process parameters were emission characteristics (CO, UBHC, NO_x, CO_2 and smoke) and performance characteristics (BTE and BSEF). Table 3 details the design matrix and the outcomes of experimental trial runs in the test engine which were the input for RSM with twenty seven experimental trials. Second order polynomial function was applied on the obtained data to analyze its coherence [21].
The developed model was assessed using the Analysis of Variance (ANOVA) regression approach to understand its suitability and to establish its empirical relationship to evaluate the output of the developed model. The synergetic effect of the input operational variables and the responsive output were assessed using RSM based on its desirability value. The pure error estimation in ANOVA was carried out with the help of center point data and lack of fit. The developed RSM model was evaluated based on the R^2, adj R^2, RMSE, MSE, MRPD, SEP and MAE values which were derived with the help of equation (1) to (7) as shown below

$$R^2 = 1 - \frac{\sum_{n=1}^{n}(y_{i,e}-y_{p,i})^2}{\sum_{n=1}^{n}(y_{p,i}-y_{e,average})^2} \quad \dots (1)$$

$$Adjusted\ R^2 = 1 - [(1-R^2)x\frac{n-1}{n-1-k}] \quad \dots (2)$$

$$MSE = \frac{1}{n}\sum_{n=1}^{n}(y_{i,p} - y_{i,e})^2 \quad \dots (3)$$

$$RMSE = \sqrt{MSE} \quad \dots (4)$$

$$MAE = \frac{1}{n}\sum_{n=1}^{n}|y_{e,i} - y_{p,i}| \quad \dots (5)$$

$$SEP = \frac{\sqrt{MSE}}{y_{e,average}} x\ 100 \quad \dots (6)$$

$$MRPD = \frac{1}{n}\sum_{n=1}^{n}\frac{|y_{e,i}-y_{p,i}|}{y_{e,i}} x\ 100 \quad \dots (7)$$

where $y_{e,average}$ and $y_{e,i}$ represented the average experimental yield and experimental yield respectively. 'k' and 'n' was the number of factors and number of trial runs respectively. $y_{p,average}$ and $y_{i,p}$ represented the average of predicted yield by RSM and predicted yield by RSM technique respectively. Similarly,.

5. Assessment of the Developed Model

Analysis of Variance (ANOVA) methodology was used to evaluate the developed RSM model by mathematical explicating the obtained p-value. The regression equation was derived using ANOVA for the developed model with respect to the output responses such as performance and emission phenomenon as detailed in Equations (8) to (14) below were A, B and C which represent the test fuel blend (FB), engine load (EL) and compression ratio (CR) respectively.

$$BTE = +27.87 + 3.09(A) + 0.2708(B) + 16.83(C) + 0.9913(AB) + 1.91(AC) - 0.0259(BC) + 0.8774(A^2) + 0.6725(B^2) - 12.15(C^2) \quad \dots(8)$$

$$BSFC = +0.3930 - 0.0579(A) - 0.0088(B) - 0.0744(C) - 0.0044(AB) - 0.0029(AC) + 0.0041(BC) + 0.0007(A^2) - 0.0175(B^2) + 0.0956(C^2) \quad \dots(9)$$

$$CO = +0.0362 - 0.0048(A) - 0.0039(B) - 0.0076(C) + 0.0003(AB) - 0.0001(AC) + 0.0013(BC) + 0.0008(A^2) - 0.0001(B^2) + 0.0060(C^2) \quad \dots(10)$$

$$UBHC = +83.90 - 6.12(A) - 4.11(B) - 9.27(C) + 1.22(AB) + 1.43(AC) + 0.3233(BC) + 3.724(A^2) + 0.0950(B^2) + 7.83(C^2) \quad \dots(11)$$

$$CO = +413.39 + 19.09(A) + 10.25(B) + 101.65(C) + 3.47(AB) + 5.49(AC) - 0.6956(BC) + 2.44(A^2) + 14.25(B^2) - 42.73(C^2) \quad \dots(12)$$

$$NO_x = +645.59 + 33.22(A) + 16.92(B) + 63.62(C) + 0.8821(AB) + 4.01(AC) + 0.3098(BC) + 8.76(A^2) - 0.8118(B^2) - 25.93(C^2) \quad \ldots(13)$$

$$Smoke = +90.23 - 3.01(A) - 1.97(B) + 4.01(C) - 0.0945(AB) + 0.3073(AC) + 0.1275(BC) + 0.1282(A^2) + 0.2304(B^2) - 0.6405(C^2) \quad \ldots(14)$$

Considering the individual p-value with its corresponding lack of fit and pure error for the performance as well as emission parameters, it can be noticed that all the outcomes of the developed model was significant with p-value closer to one. The RSM experimental design and the statistical regression data of the developed RSM model is tabulated in Table 5 and Table 6 respectively. The ANOVA factors like goodness of prediction (adj R^2), goodness of fit (R^2) and its corresponding prediction was found to be significant. 'R^2' denotes the cumulative variation in the RSM model after prime factor consideration, whereas 'adj R^2' denotes the cumulative prediction inherent in the RSM model. The evaluative outcomes of the R^2 and adj R^2 closer to unity makes the developed model to be a perfect fit, whereas the value closer to zero indicate its in-significance and expels the model from being used or applied [22]. Here, the R^2 and adj R^2 values of the emission and performance models were closer to unity ranging between 0.8375 and 0.9868 and make it the best suited for the suggested analysis.

6. Results and Discussion

6.1. Brake Thermal Efficiency

Brake thermal efficiency is represented in 3D surface plots using RSM in which it is plotted in three ways. Three main factors such as fuel blend ratio, engine load and compression ratio are used to analyse the brake thermal efficiency. Figure 3A represents the BTE influenced by fuel blend ratio and engine load. Figure 3B denotes the optimal BTE which is influenced by compression ratio and engine load. Figure 3C portrays the variations of BTE with respect to compression ratio and fuel blend ratio. As can be seen in Figure 3A, brake thermal efficiency was predicted to be drastically low at low load conditions for mineral diesel. This may be due to insufficient combustion temperature prevalent inside the combustion chamber which led to incomplete combustion by poor atomization. On the other hand, D80PSBD20 had a slightly higher brake thermal efficiency when compared to mineral diesel. D80PSBD20DEE10 had better BTE when compared to the D80PSBD20 fuel blend. BTE values escalated on increase in engine load conditions up to 9 kg which was nearly 80% of the engine load condition. At this load conditions the temperature inside the cylinder increased as more amount of fuel was burnt. At optimal load conditions, D80PSBD20DEE10 achieved the maximum brake thermal efficiency.

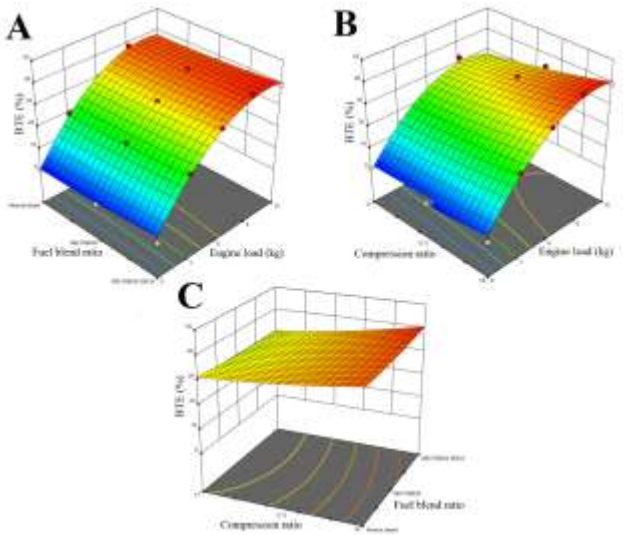

Fig 3. Variation in BTE due to EL and FB (A), EL and CR (B) and FB and CR

In Figure 3B, brake thermal efficiency was analysed using the compression ratios 17:1, 17.5:1 and 18:1 and engine loads. Initially, the BTE was low at low-load conditions at compression ratio 17:1. At 18CR, the volume of the combustion chamber was reduced to create higher in-cylinder pressure during combustion which led to complete combustion. As can be seen in Figure 3C, compression ratio and fuel blend ratio influenced the BTE with increase in CRS and fuel blends. At 17CR, least value of BTE was observed for all test fuels and at 17.5CR, there was a slight improvement in BTE compared to 17CR for all test fuels. Maximum BTE was achieved at 18CR and D80PSBD20DEE10 fuel blend which may be due to increase in oxygen content and flammable characteristics presented in the oxygenated additives which was aided by the increase in viscosity and calorific value of the PSBD. D80PSBD20DEE10 fuel blend had DEE oxygenated additives which improved the BTE. D80PSBD20DEE10 fuel blend had the high calorific value as 45179kJ/kg compared to two test fuels. At 18CR, the optimal BTE was observed as high in-cylinder pressure was present inside the combustion chamber. Moreover, 9.55229kg was predicted as an optimal load which produced the high BTE which may be due to complete combustion. The corresponding loads were 80% of the engine loads. After increase beyond the optimal load condition, the BTE was observed to decrease drastically. Higher brake thermal efficiency was predicted as 41.78% for D80PSBD20DEE10 fuel at 18CR and 9kg load condition. On the other hand, lower BTE was observed for mineral diesel at 17.5CR and 3kg load condition. The optimal value was generated based on the RSM plots and ANNOVA table (refer Table No 5). Finally, the optimal values of the parameters as predicted by RSM was compression ratio 18:1, D80PSBD20DEE10 fuel blend and 9.55229 kg load which produced an optimal brake thermal efficiency as 40.5663%. The findings were also similar to Umit et al.[27] and Hayder et al. [20].

Table 5. RSM design table with experimental data's of emission and performance parameters

Run order	CR	Load (Kg)	Fuel blend	BSFC (kg/kWhr)	BTE (%)	UBHC (ppm)	CO_2 (g/kWhr)	NO_x (ppm)	CO (%)	Smoke (%)
1	17	0	0	0.6	0	115	270	530	0.059	91
2	17	6	0	0.45	24.83	99	350	583	0.048	95
3	17	12	0	0.47	31.25	95	410	625	0.044	99
4	17	0	1	0.62	0	108	280	538	0.052	89
5	17	6	1	0.47	22.78	94	360	605	0.045	94
6	17	12	1	0.49	27.85	92	430	645	0.043	96
7	17	0	2	0.58	0	102	310	550	0.048	87
8	17	6	2	0.43	23.52	88	370	620	0.042	92
9	17.5	12	2	0.45	29.65	86	450	665	0.039	93
10	17.5	0	0	0.53	0	99	310	561	0.056	89
11	17.5	6	0	0.38	28.96	93	410	604	0.042	93
12	17.5	12	0	0.4	34.78	91	482	645	0.04	95
13	17.5	0	1	0.56	0	97	270	578	0.049	84
14	17.5	6	1	0.41	26.71	88	359	622	0.038	90
15	17.5	12	1	0.43	32.54	86	440	662	0.035	94
16	17.5	0	2	0.52	0	94	290	589	0.044	84
17	17.5	6	2	0.37	28.23	83	389	641	0.033	89
18	17.5	12	2	0.39	34.45	81	462	685	0.032	91
19	18	0	0	0.5	0	96	280	578	0.048	85
20	18	6	0	0.35	30.28	85	380	640	0.038	88
21	18	12	0	0.37	36.1	83	445	695	0.035	93
22	18	0	1	0.49	0	93	302	597	0.045	82
23	18	6	1	0.33	32.25	82	410	660	0.035	87
24	18	12	1	0.35	37.56	80	462	712	0.034	92
25	18	0	2	0.47	0	89	330	620	0.04	81
26	18	6	2	0.31	34.47	79	430	680	0.03	86
27	18	12	2	0.33	39.4	77	510	736	0.028	89

Table 6. RSM model evaluation

Model	BSFC	BTE	CO	CO_2	NO_x	UBHC	Smoke
R^2	0.9401	0.9868	0.8613	0.866	0.8375	0.8108	0.9784
Predicted R^2	0.9024	0.9773	0.7783	0.6268	0.7472	0.7056	0.9645
AdjR^2	0.9247	0.9834	0.8257	0.7059	0.7957	0.7622	0.9728
SD	0.0235	1.75	0.0036	48.41	28.04	5.27	0.6794
Mean	0.4282	29.92	0.0396	400.58	638.58	88.04	90.09
Model degree	Quadratic	Quadratic	Quadratic	Quadratic	Quadratic	Quadratic	Quadratic

6.2. Brake Specific Fuel Consumption

BSFC is the vital factor for deciding the engine efficiency. Here, three surface plots based on RSM technique was used to determine the brake thermal efficiency using three significant parameters. Again, three focal factors such as compression ratio, fuel blend proportion and engine load were deployed to analyze the brake specific fuel consumption. Fuel blend ratio and engine load influenced the BSFC as denoted in Figure 4A. In Figure 4B, BSFC was influenced by engine load and compression ratio. Figure 4C illustrates the influence of compression ratios and fuel blend ratios on BSFC. Figure 4A showed the considerably low BSFC of the engine for the D80PSBD20DEE10 fuel blend at 9.55229kg load conditions. Higher BSFC was predicted at low load conditions when fuelled with mineral diesel. The decrease in BSFC with load was due to increase in temperature and pressure inside the combustion chamber

which in turn improved the combustion thereby reducing the fuel consumption [21]. D80PSBD20 had a slightly higher value of BSFC when compared to D80PSBD20DEE10. Figure 4B highlights the 3D surface plot of BSFC by changing the CRS as 17:1, 17.5:1 and 18:1 and the variations of engine loads from 0 to 12 kg. The optimal BSFC was observed at 18:1 compression ratio which was due to decrease in volume of cylinder which led to high pressure and reducing the consumption of fuel. At 17.5CR, the amount of fuel consumption was slightly increased. The optimal BSFC was attained at 9.55229kg load which was 80% load of the engine load as it increased the temperature inside the cylinder, and it helped to burn the fuel. The reduction of fuel consumption with CR was due to higher cylinder pressure at higher compression ratio. Figure 4C portrays the BSFC by altering the compression ratios and fuel blend ratios. The optimal BSFC was achieved for D80PSBD20DEE10 fuel blend which had diethyl ether content as oxygenated additives. The oxygenated additives had flammable characteristic and it helped to improve the viscosity and calorific value of the base fuel. The optimal BSFC was observed to be 0.285362 kg/kWhr based on compression ratio 18:1 at 9.55229 kg engine load for D80PSBD20DEE10 fuel blend as analyzed by RSM techniques. Highest value of BSFC was predicted to be as 0.62kg/kWhr at 17CR for D80PSBD20 fuel blend at 0 load condition. The lowest amount of BSFC was found to be as 0.28 kg/kWhr at 18CR for D80PSBD20 fuel blend at 9kg load condition [23, 24].

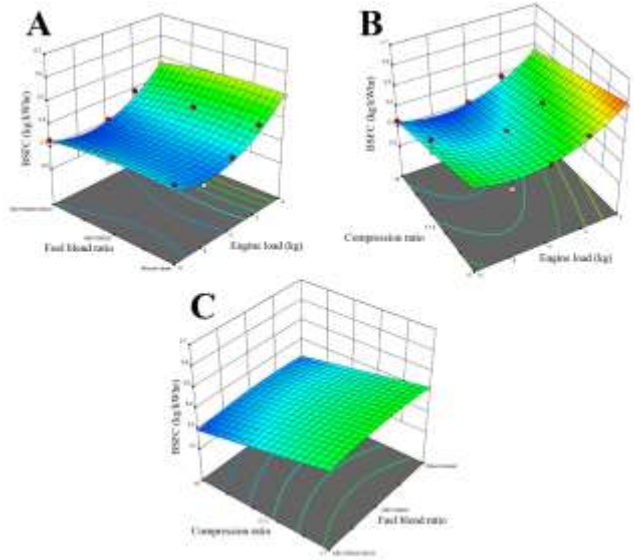

Fig 4. Variation in BSFC due to EL and FB (A), EL and CR (B) and FB and CR

6.3. CO Emission

Carbon monoxide emission is a prominent factor in the emission characteristics and CO emission is explained using 3D surface plots generated by RSM technique. The 3D surfaces plots is generated based on three core input factors such as compression ratio, engine loads and fuel blend ratio. Figure 5A shows the CO emission affected by fuel blend ratios and engine loads. Five different loading conditions was applied on the CI engine(0kg, 3kg, 6kg, 9kg and 12kg) and three fuel blends was used in the experiments (mineral diesel, D0PSBD20 and D80PSBD20DEE10). Initially, higher CO emission was predicted at no load when fueled with mineral diesel which was due to incomplete combustion and poor conversion of energy. Lower value of CO emission was observed at 9.55229kg load which was considered to be as optimal load condition as predicted by the RSM technique. The focal reason for CO emission owes to lack of enough oxidation temperature at the later part of combustion. Figure 5B depicted the CO emission characteristics influenced by the changing compression ratios and engine loads. The reduction of CO emission with rise in CR was due to the escalation in temperature and pressure with CR. High CR and high loads delivered oxidation temperature which helped in reduction of the CO emission. The peak CO emission was observed at 17 CR which was due to lack of temperature and pressure [22]. At 18:1 CR, the CO emission showcased the low CO emission. As can be seen in Figure 5C, the compression ratio and fuel blend ratio influenced the CO emission.

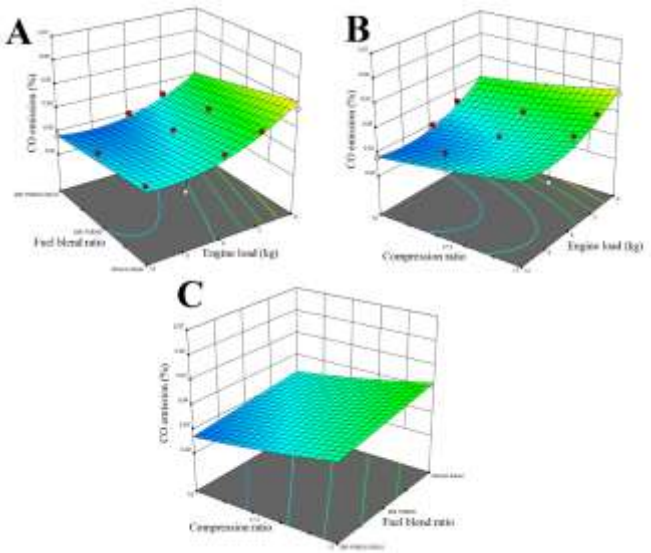

Fig 5. Variation in CO emission due to EL and FB (A), EL and CR (B) and FB and CR

The optimal CO emission was predicted at 18:1 compression ratio and D80PSBD20DEE10 fuel blend. Using this fuel blend which had 10% of diethyl ether gave the extra amount of oxygen which helped to improve the brake thermal efficiency and droop in the CO emission. Due to its better fuel property, D80PSBD20DEE10 fuel blend gave a better performance. The properties of D80PSBD20DEE10 fuel blend and mineral diesel were slightly lower which led to increase the CO emission. Higher value of CO emission was produced as 0.059% at 17:1 compression ratio for mineral diesel as a fuel at low load condition. The lowest CO emission was obtained as 0.023% at 18:1 compression ratios for D80PSBD20DEE10 fuel blend at 9kg load condition. Finally, the optimal CO emission was recorded as 0.027002% with D80PSBD20DEE10 fuel blend at 18:1 compression ratio at 9.55229kg load conditions.

6.4. UBHC Emission

Un-burnt hydrocarbon is a cardinal parameter in the engine emission phenomenon. In general, UBHC is released from the variable compression ratio direct injection compression ignition engine because of lower combustion temperature and pressure along with lean or rich mixture. Figure 6A explains the influence of engine load and fuel blend ratio on UBHC emission. Initially, high value of UBHC emission was predicted at low load condition. On addition of load up to 9 kg load condition, the UBHC emission attained a lesser value due to the effect of fuel viscosity and fuel spray quality inside the combustion chamber. The optimal UBHC was achieved at 9.55229 kg which was 80% of engine load. Figure 6B portrayed the UBHC emission influenced by fuel blends (mineral diesel, D80PSBD20 and D80PSBD20DEE10) and compression ratios. D80PSBD20DEE10 fuel owed a significant fuel property when compared to mineral diesel. D80PSBD20DEE10 fuel blend had additional benefits in terms of oxygenated additives as DEE. Owing to addition of 10% DEE into the D80PSBD20 fuel enhanced the combustion which led to low UBHC emission formation [26]. The optimal UBHC was reached when fueled with D80PSBD20DEE10 blend.

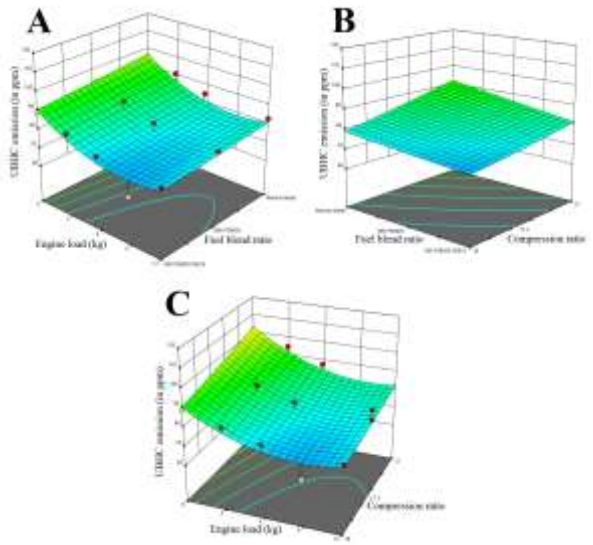

Fig 6. Variation in UBHC emission due to EL and FB (A), EL and CR (B) and FB and CR

This was due to availability of additional oxygen in the fuel blend. Figure 6C illustrates the variations of compression ratio and loads on UBHC emission. At 17:1CR, the UBHC emission was observed to be drastically high. UBHC emission became lower value when the compression ratio was increased up to 18:1 CR. The optimal UBHC emission was attained as 73.65 ppm at 18:1CR and 9.55229 load condition for D80PSBD20DEE10 fuel blend. In general, as the CR was increased from 17:1 to 18:1 CR, it resulted with high temperature and additional oxygen content present in the fuel blends improved the combustion process resulting in greater reduction of UBHC emissions with increase in engine loads [23]. Higher value of UBHC was predicted as 115ppm at 17:1 CR for mineral diesel as a fuel at full load conditions. The lower UBHC emission was observed to be as 68ppm with D80PSBD20 as fuel blend at 18:1CR at 9 kg load conditions.

6.5. CO_2 Emission

The 3D surface plots generated by RSM technique involving CO_2 emission for engine load with fuel blend ratio, engine load with compression ratio, and fuel blend combined with compression ratio is discussed here. Figure 7A showcase the CO_2 emission with respect to engine loads and fuel blend ratios. The maximum CO_2 emission was observed at 9kg load for D80PSBD20DEE10 fuel blend which was due to complete combustion that occurred inside the combustion chamber. Generally, CO_2 was recognized as product of complete combustion. At 9.55229 kg load, the optimal CO_2 emission was observed with engine parameters playing a supporting role with escalation of temperature inside the combustion chamber. Figure 7B illustrates the CO_2 emission with respect to engine loads and compression ratios. Compression ratio was observed to be the noticeable factor in this study and 18:1 CR enhanced the CO_2 emission with load conditions. 18:1 CR was used to improve the combustion characteristics thereby increasing the CO_2 emissions [19, 21]. At 17:1 and 17.5:1 CRS, the low CO_2 emission was predicted which was due to insufficient temperature prevalent inside the combustion chamber. The optimal CO_2 emission was observed at 18CR and 9.55229kg load conditions. Figure 7C represented the CO_2 emission as influenced by fuel blend and compression ratios. D80PSBD20DEE10 fuel produced a significant amount of CO_2 emission which was due to presence of enough oxygen content inside the combustion chamber. Mineral diesel and D80PSBD20 fuel blends gave a lower amount of CO_2 emission indicating incomplete combustion and insufficient supply of oxygen.

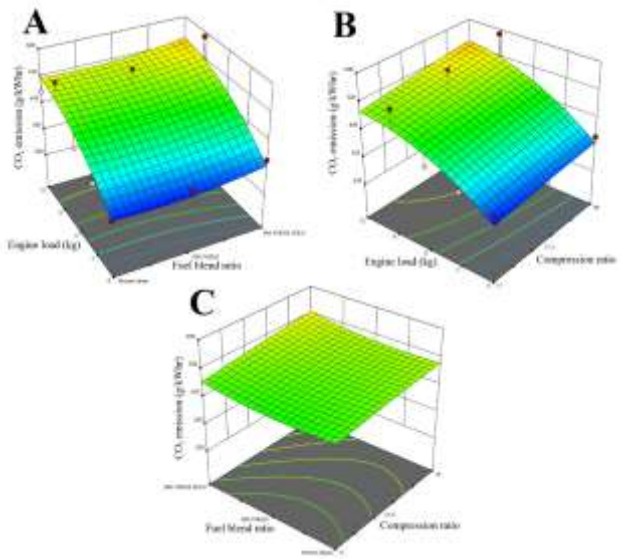

Fig 7. Variation in CO_2 emission due to EL and FB (A), EL and CR (B) and FB and CR

The lower amount of CO_2 emission was observed to be as 270 g/kWhr for mineral diesel as a fuel at 17:1CR and low load conditions. The maximum amount of CO_2 emission was predicted to be as 583 g/kWhr when fuelled with D80PSBD20DEE10 fuel blend at 18:1 CR and 9kg load condition. The optimal CO_2 emission was accomplished using D80PSBD20DEE10 fuel blend as 506.32 g/kWhr at 18:1CR and 9.55229kg load conditions.

6.6. NO_x Emission

NO_x emission was formed by oxidation due to prevalent of high temperature inside the engine cylinder. The formation of oxides of nitrogen depends on cylinder temperature and oxygen content. Figure 8A denoted the NOx emission influenced by the engine loads with fuel blend ratios. Figure 8B illustrates the NOx emission influenced by the engine loads and compression ratios. Figure 8C showcased the oxides of nitrogen emission as influenced by fuel blend ratios and compression ratios. As can be seen in Figure 8A, the lowest value of NOx emission was reported for mineral diesel and D80PSBD20 fuel blend at lower loading conditions. By increasing the load up to 80% load, highest NOx emission was determined for D80PSBD20DEE10 fuel blend. Optimal value of NOx emission was determined at the optimal load condition of 9.55229 kg using RSM technique. Figure 8B showed the formation of NOx inside the combustion chamber at high temperature and pressure at high loads and higher compression ratios. At the initial stage of operation at 17:1 CR, the NOx emission was very low due to lower cylinder pressure resulting into lower temperature inside the combustion chamber [26]. After it was increased to 18:1 CR, the formation of the NOx emission was higher due to higher cylinder pressure inside the combustion chamber. As can be seen in Figure 8C, the emission of NOx for D80PSBD20DEE10 fuel blend was higher with increase in load conditions.

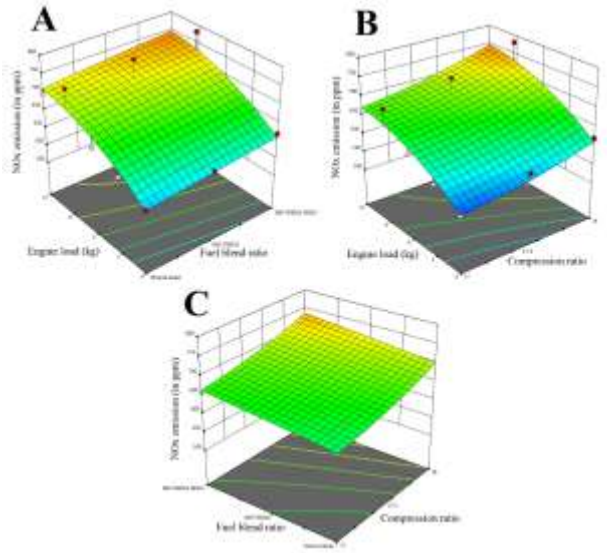

Fig 8. Variation in NO_x emission due to EL and FB (A), EL and CR (B) and FB and CR

Oxygen content present in the biodiesel helped with better combustion and rate of heat release was high which escalated the NOx emission. D80PSBD20DEE10 fuel blend had an extra 10% of oxygen which aid in the formation of NO_x. The lowest value of NOx emission was observed to be as 530 ppm for mineral diesel at 17:1 CR and no load condition. The highest value of NOx emission was observed to be as 780 ppm at 18:1CR for D80PSBD20DEE10 fuel blend at 9kg load condition. The optimal NOx emission was recorded as 735.721 ppm at 18:1CR using D80PSBD20DEE10 as a fuel at 9.55229kg load conditions.

6.7. Smoke Emission

In general, smoke is numerous solid unburnt hydrocarbon particles produced during the combustion process. Smoke opacity was determined using 3D surface plots generated from response surface methodology technique for engine load with compression ratio, fuel blend ratio and engine load with fuel blend. Viscosity, density and rich air-fuel ratio factors are the main factors causing smoke formation. Generally, biodiesel oxidises the unburned HC and reduces smoke formation due to its high volatility. Lower smoke emission was predicted for D80PSBD20DEE10 fuel blend at 9kg load condition (refer Figure 9A). But, higher values of smoke opacity were observed at low load conditions. At part load conditions, the smoke values ranged in-between the values of low and high smoke emissions. By increasing the load up to 9kg, the smoke reduced due to prevailing sufficient in-cylinder pressure generated with increase in the load conditions. As can be seen in Figure 9B, smoke emission was analysed by changing the compression ratio and loads. In this process, the variation of CR such as 17:1, 17.5:1 and 18:1 CR helped to increase or decrease the volume of combustion chamber. At 17:1 CR, the volume of combustion chamber increased leading to low combustion characteristics [27, 28]. At 18:1 CR, the volume of combustion chamber decreased which led to higher cylinder pressure inside the combustion chamber. Therefore, the smoke formation reduced. As can be seen in Figure 9C, the optimal value of smoke emission achieved for D80PSBD20DEE10 fuel blend due to additional oxygen content present in the fuel which reduced the soot nucleate process.

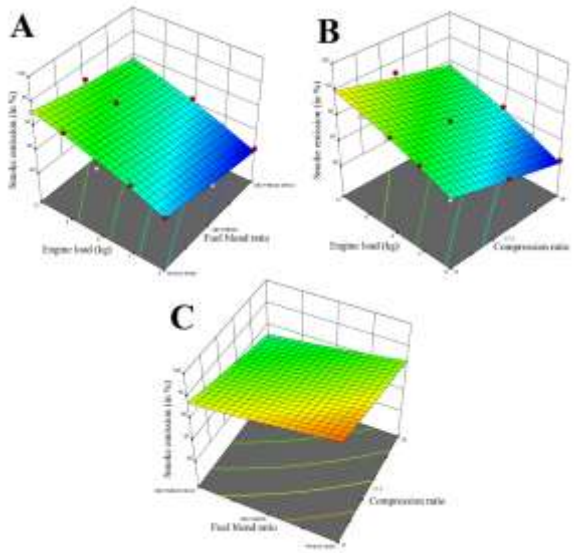

Fig 9. Variation in Smoke emission due to EL and FB (A), EL and CR (B) and FB and CR

Finally, the optimal value of smoke opacity was observed to be as 89.9334% with D80PSBD20DEE10 fuel blend at 18CR and 9.55229kg load condition. The lower value of smoke opacity was analysed to be as 82% with D80PSBD20DEE10 fuel blend at 18:1 compression ratio and no load conditions. The higher value of smoke emissions was observed to be as 99% for mineral diesel at 17:1 compression ratio at 12 kg load conditions.

Table 7. Desirability value of the developed RSM model

CR	1
Fuel blend	1
Load	1
BTE	0.970951
BSFC	0.927538
CO	0.00007
UBHC	0.826924
CO_2	0.754097
NOx	0.822885
Smoke	0.614809
Combined	0.821523

Table 8. RSM optimization with respect to input variables and output responses

CR	18
Fuel blend	D80PSBD20DEE10
Load(kg)	9.55229
BTE (%)	40.5663
BSFC (kg/kWhr)	0.295362
CO (%)	0.270002
UBHC (ppm)	73.65
CO_2(g/kWhr)	506.32
NOx(ppm)	735.721
Smoke (%)	87.9334

Table 7 illustrates the desirability value of the developed RSM model with respect to the variable input parameters and RSM output responses. It can be noticed that the input variables had acquired unity as desirability value which was very much favourable for the test conditions. The output responses varied between 0.970951 and 0.614809 with CO having 0.00007 as desirability value. The RSM approach illustrated the synergetic effect fuel blend ratio, compression ratio and engine load along with output responses was established in detail. Table 8 details the optimized engine input parameters during which the maximum performance can be obtained with minimal exhaust emissions. RSM predicted the maximum brake thermal efficiency for CR18:1 at 9.55229kg engine load for D80PSBD20DEE10 fuel blend as 40.5663% at 0.295362 kg/kWhr brake specific fuel consumption [29, 30]. The exhaust emission were estimated as 0.270002% of CO, 73.650 ppm of UBHC, 506.36 g/kWhr of CO_2, 735.721 ppm of NO_x and 87.9334% of smoke emission. All the outcomes were in-line with the experimental results.

7. Conclusion

In the present study, the optimization of diesel engine input variable parameters when fuelled with oxygenated blends of palm stearin biodiesel was evaluated using RSM approach. It was noticed that the input operating conditions namely fuel blend, compression ratio and engine load significantly influenced the performance and exhaust emissions. Experimental trials runs were conducted based on the DOE full factorial design of twenty seven runs and the synergetic effect between the input variables parameters were assessed in detail. Based on the outcomes of the study, following conclusions were arrived.

- Base catalyzed transesterification process with Methanol and NaOH transformed the palm stearin wax into its biodiesel at molar ratio 1:6, 0.54 wt% of NaOH catalyst and 12 minutes reaction duration with transesterification efficiency of 96.5%. The properties of the derived biodiesel and the formulated test fuel blends were in accordance with the ASTM limits.
- The developed RSM model with the help of CCRD design matrix was found to be significant with 98.6% confidence level.
- Higher BTE was observed with at CR of 18:1. Increasing the concentration of DEE to diesel-biodiesel blends further augmented the BTE up to 41.78% at $3/4^{th}$ loading conditions.
- BSFC portrayed a significant reduction on increase in compression ratio from 17:1 to 18:1. CR18:1 exhibited a lower BSFC for D80PSBD20DEE10 at part load condition.
- Mineral diesel-palm stearin biodiesel-DEE concentration significantly affected the levels of UBHC and CO emission in the exhaust at all CR and loading conditions. CR17:1 exhibited a higher UBHC and CO emission as 115 ppm and 0.059% at low load, whereas lower UBHC and CO emission was seen at CR18:1 as 68 ppm and 0.023% respectively at $3/4^{th}$ engine load. Optimal concentration of UBHC and CO was seen at CR18:1 for oxygenated fuel blends at 9.55229 kg engine load.

- NO_x emission was seen at higher level for D80PSB20DEE10 fuel blend at CR17.5:1 and 18:1 during part and full loads, whereas D80PSB20 recorded a lower NO_x due to reduced flame temperature. Higher NO_x of 780 ppm was observed for D80PSB20DEE10 at CR18:1 during part load condition.
- Based on the desirability value and RSM prediction, the optimal input operation parameters were CR18:1, D80PSBD20DEE10 blend and 9.55229 kg of engine load. The optimal output response for BTE, BSFC, CO, UBHC, CO_2, NO_x and smoke were 40.5663%, 0.295362 kg/kWhr, 0.27002%, 73.65 ppm, 506.32 g/kWhr, 735.721 ppm and 87.9334% respectively.

Finally, it can be concluded that careful controlling of the input operational parameters improved the efficiency of the engine significantly. The suggested RSM model could also be effectively used in other diesel engine to understand its ability and accuracy. The usage of palm stearin wax, an agriculture residual waste, as fuel in diesel engine can be supplemented along with oxygenated additives to close the carbon chain and minimize global warming. Moreover, the use of palm stearin wax also attribute to the country's economy as well. In future to understand the combustion behavior better, the injection timing and injection pressure may be varied while testing. Similarly to reduce the NO_x values EGR may be tried to understand the reduction of emission concept while studying the combustion behavior also.

References

[1] Osmano Souza Valente, Marcio Jose da Silva, Vanya Marcia Duarte Pasa, Carlos Rodrigues Pereira Belchior, Jose Ricardo Sodre. Fuel consumption and emissions from a diesel power generator fuelled with castor oil and soybean biodiesel. Fuel 89 (2010) 3637–3642.

[2] Gopinath Dhamodaran, Ramesh Krishnan, Yashwanth Kutti Pochareddy, Homeshwar Machgahe Pyarelal, Harish Sivasubramanian, Aditya Krishna Ganeshram. A comparative study of combustion, emission, and performance characteristics of rice-bran-, neem-, and cottonseed-oil biodiesels with varying degree of unsaturation. Fuel 187 (2017) 296–305

[3] Hariram V, Seralathan S, Dinesh Kumar M, Vasanthaseelan S and Sabareesh M. Analyzing the fatty methyl ester profile of palm kernel biodiesel using GC/MS, NMR and FTIR techniques, Journal of Chemical and Pharmaceutical Sciences 9(4) (2016) 3122-3128.

[4] Hariram V, Seralathan S, Kunal Bhutoria and Harsh H Vora. Experimental study on combustion and performance characteristics in a DI CI engine fuelled with blends of waste plastic oil, Alexandria Engineering Journal 57 (2018) 2257 – 2263.

[5] Hariram V, Prakash S, Seralathan S and Micha Premkumar T. Data set on optimized biodiesel production and formulation of emulsified Eucalyptus teriticornisis biodiesel for usage in compression ignition engine. Data in Brief 20 (2018) 6-13.

[6] Dimitrios C. Rakopoulos, Constantine D. Rakopoulos, Evangelos G. Giakoumis, Roussos G. Papagiannakis, Dimitrios C, Kyritsis. Influence of properties of various common bio-fuels on the combustion and emission characteristics of high-speed DI (direct injection) diesel engine: Vegetable oil, bio-diesel, ethanol, n-butanol,diethyl ether. Energy 73 (2014) 354-366.

[7] Ashok Kumar T, Chandramouli R, Mohanraj T. A study on the performance and emission characteristics of esterified pinnai oil tested in VCR engine. Ecotoxicol. Environ. Saf. (2015), http://dx.doi.org/10.1016/j.ecoenv.2015.06.008.

[8] Ambarish Datta and Bijan Kumar Mandal. A numerical study on the performance, combustion and emission parameters of a compression ignition engine fueled with diesel, palm stearin biodiesel and alcohol blends. Clean Techn Environ Policy (2016), DOI 10.1007/s10098-016-1202-3.

[9] Ganesh R, Manikandan K and Jishu Chandran. Emission analysis of palm stearin biodiesel fueled diesel engine. International Journal of Ambient Energy (2018), DOI:10.1080/01430750.2018.1517692.

[10] Pali Rosha, Saroj Kumar Mohapatra, Sunil Kumar Mahla, HaengMuk Cho,Bhupendra Singh Chauhan, Amit Dhir. Effect of compression ratio on combustion, performance, and emission characteristics of compression ignition engine fueled with palm (B20) biodiesel blend. Energy 178 (2019) 676-684.

[11] Prakash T, Edwin Geo V, Leenus Jesu Martin, Nagalingam B. Effect of ternary blends of bio-ethanol, diesel and castor oil on performance, emission and combustion in a CI engine. Renewable Energy 122 (2018) 301-309.

[12] Patil KR, Thipse SS. Experimental investigation of CI engine combustion, performance and emissions in DEE–kerosene–diesel blends of high DEE concentration. Energy Conversion and Management 89 (2015) 396–408.

[13] Anand R, Mahalakshmi NV. Simultaneous reduction of NOx and smoke from a direct-injection diesel engine with exhaust gas recirculation and diethyl ether. Proc Inst Mech Engrs Part D: J Automob Eng 2007;221. doi.10.1243/09544070JAUTO258

[14] Muralidharan K, Vasudevan D, Sheeba KN. Performance, emission and combustion characteristics of biodiesel fueled variable compression ratio engine. Energy 36 (2011) 5385-5393.

[15] Vikas Sharma, Ganesh Duraisamy, Kanagaraj Arumugum. Impact of bio-mix fuel on performance, emission and combustion characteristics in a single cylinder DICI VCR engine. Renewable Energy 146 (2020) 111-124

[16] Sakthivel R, Ramesh K, Joseph John Marshal S, Kishor Kumar Sadasivuni. Prediction of performance and emission characteristics of diesel engine fueled with waste biomass pyrolysis oil using response surface methodology. Renewable Energy 136 (2019) 91-103

[17] Datta Bharadwaz Y, Govinda Rao B, Dharma Rao V, Anusha V. Improvement of biodiesel methanol blends performance in a variable compression ratio engine using response surface methodology. Alexandria Eng. J. 55(2) (2016) 1201-09.

[18] Pandian. M, S.P. Sivapirakasam, M. Udaykumar, Investigation on the effect of injection system parameters on performance and emission characteristics of a twin cylinder compression ignition direct injection engine fueled with Pongamia biodiesel–diesel blend using response surface methodology, Appl. Energy 88 (2011) 2663–2676.

[19] Amger Al Ezzi, Mohammed A. Fayad, Ayad M. Al Jubori, Alaa Abdulhady Jaber, Laith A Alsadawi, Hayder A. Dhahad, Miqdam T. Chaichan, Talal Yusaf. Influence of fuel injection pressure and RME on combustion, NO_x emissions and soot nanoparticle in common-rail HSDI diesel engine, International Journal of Thermofluids 15 (2022) 100173.

[20] Hayder A. Dhahad, Mohammed A. Fayad, Moqdam T. Chaichan, Alaa Abdulhady Jaber, Megaritis T. Influence of fuel injection timing strategies on performance, combustion, emission and particulate matter characteristics fueled with rapeseed methyl ester in modern diesel engine. Fuel 306 (2021) 121589.

[21] Mohameed A. Fayad, Ali Ooda Abd, Miqdam T. Chaichan, Hayder A. Dhahad, Amged Al Exxi. Investigation the combined effects of exhaust gas recirculation (EGR) and alcohol-diesel blends in improvement of NOx-PM trade-off in compression ignition (CI) diesel engine. IOP Conf. Series: Earth and Environment Science 961 (2022) 012048.

[22] S. Dewang, S. Suriani, Hadriani, Diana, E. S. Lestari and Bannu. "Viscosity and calorie measurements of biodiesel production from *Calophyllum Inophyllum* L using catalyst and time variations for stirring in transesterification process" 2017 IEEE 6th International Conference on Renewable Energy Research and Applications (ICRERA), pp. 734-738. 2017

[23] Hariram V and Vasanthaseelan S. Optimization of Base catalysed Transesterification and Characterization of Brassica napus (Canola seed) for the production of Biodiesel, International Journal of ChemTech Research 8(9) (2015) 418 – 423.

[24] Hariram V, John J Godwin, Seralathan S, Micha Premkumar T. Comparative analysis of combustion, performance and emission phenomenon of a CI engine fuelled with algal and cotton seed biodiesel, International Journal of Ambient Energy 42(6) (2021) 636-647.

[25] Alpaslan Atmanl, Bedri Yuksel, Erol Ileri, Deniz Karaoglan A. Response surface methodology-based optimization of diesel–n-butanol–cotton oil ternary blend ratios to improve engine performance and exhaust emission characteristics. Energy Conversion and Management 90 (2015) 383–394.

[26] E.K. Çoban, C. Gençoğlu, D. Kirman, O. Pinar, D. Kazan and A.A. Sayar. "Assessment of the effects of medium composition on growth, lipid accumulation and lipid profile of Chlorella vulgaris as a biodiesel feedstock" 2015 International Conference on Renewable Energy Research and Applications (ICRERA), pp. 793-796. 2015.

[27] Umit Agbulut, Mustafa Ayyıldız, Suat Sarıdemir. Prediction of performance, combustion and emission characteristics for a CI engine at varying injection pressures. Energy 197 (2020) 117257.

[28] S.A. Abd Allah. El-Gharabawy. "Cost Analysis for Biodiesel Production from Waste Cooking Oil Plant in Egypt" International Journal of Smart Grid, ijSmartGrid, 1(1), pp. 16-25. 2017.

[29] Y. Tominaga, M. Tanaka, H. Eto, Y. Mizuno, N. Matsui and F. Kurokawa. "Design Optimization of Renewable Energy System Using EMO" 2018 International Conference on Smart Grid (icSmartGrid), pp. 258-263. 2018.

[30] R. Arslan and Y. Ulusoy. "Utilization of waste cooking oil as an alternative fuel for Turkey," 2016 IEEE International Conference on Renewable Energy Research and Applications, pp. 149-152. 2016.